

## Oxidation behavior of $(\text{Al}_2\text{OC})_{1-x}(\text{AlN})_x$ and AlN in TG–DTA

Takeshi Tsuchida\*, Yasunori Azuma

*Division of Materials Science and Engineering, Graduate School of Engineering, Hokkaido University, North 13 West 8, Kita-ku, Sapporo 060, Japan*

Accepted 17 May 1999

### Abstract

The oxidation behavior of a commercial AlN and  $(\text{Al}_2\text{OC})_{1-x}(\text{AlN})_x$  ( $x \neq 0.80$ ), which was obtained by the self-combustion reaction induced by the mechanical activation of the powder mixtures of aluminum metal with natural graphite, was compared in TG–DTA runs. A weight increase due to the oxidation of a commercial AlN began at temperatures above 600°C, followed by a very slow increase with increasing temperature up to 1000°C, whereas that of  $(\text{Al}_2\text{OC})_{1-x}(\text{AlN})_x$  began at temperatures above 700°C, followed by a rapid increase in temperature range from 850°C to 1000°C. The fractional conversion estimated by assuming the weight increase up to 1000°C in TG corresponding to the oxidation reaction of AlN or  $(\text{Al}_2\text{OC})_{1-x}(\text{AlN})_x$  to  $\text{Al}_2\text{O}_3$  was about 8% and 23%, respectively. The difference in oxidation reactivity of AlN and  $(\text{Al}_2\text{OC})_{1-x}(\text{AlN})_x$  is discussed. © 1999 Elsevier Science B.V. All rights reserved.

*Keywords:* TG–DTA; Oxidation reaction; Aluminum nitride;  $(\text{Al}_2\text{OC})_{1-x}(\text{AlN})_x$ ; Mechanical activation

### 1. Introduction

Aluminum nitride (AlN) and AlN-based materials such as aluminum oxynitride (AlON), aluminum oxycarbide ( $\text{Al}_2\text{OC}$ ) and aluminum oxynitride carbide (AlONC) have attracted attention in advanced ceramics [1]. Recently, we have proposed a novel method for producing nitrides and carbides of aluminum [2–6], zirconium [7] and niobium [8] in air. This process is based on self-combustion reaction induced by exposing the metal (Al, Zr, Nb)–graphite (C) powder mixtures after mechanical activation by grinding in air. From the measurements of XPS spectra and the lattice constants, it was found that the aluminum

nitride obtained was solid solution between AlN and  $\text{Al}_2\text{OC}$  having a wurtzite structure, designated as  $(\text{Al}_2\text{OC})_{1-x}(\text{AlN})_x$ . The  $x$ -values changed from 0.80 [2] to 0.97 [6] depending on the reaction vessel used. This solid solution is promising as an advanced material because of its mechanical strength and toughness and its thermal and electrical properties [9–12]. Then, in order to obtain more information for practical applications, in the present paper the oxidation behavior of  $(\text{Al}_2\text{OC})_{1-x}(\text{AlN})_x$  and a commercial AlN is compared for the first time in TG–DTA experiments.

### 2. Experimental procedures

The procedures of mechanical activation of Al–C powder mixtures have been in detail described in the previous papers [2–6]. The powders of aluminum

\*Corresponding author. Tel.: +81-11-706-6578; fax: +81-11-706-6578  
E-mail address: tsuchida@eng.hokudai.ac.jp (T. Tsuchida)

metal (particle size varying between 61 and 104  $\mu\text{m}$ , 99.9% purity, Kojundo Chemical Laboratory) and natural graphite (mean flake size 5  $\mu\text{m}$ , 97% carbon, 2% ash and 1% volatile component, Nippon Kokuen Industry) were mixed in a molar ratio of  $\text{Al/C} = 3/1$  and then ground in air for 30 min in a p-7 planetary ball mill (Fritsch, Idar-Oberstein, Germany). When the ground sample was transferred into a graphite crucible (inner diameter of 30 mm and depth of 40 mm) and exposed to air, they self-ignited instantly and the exothermic reactions propagated into the powders. As soon as the reactions started, the graphite crucible was covered with another one to prevent the sample from oxidizing. After the reaction, the surface of the product lump was removed and the bulk was ground in an agate mortar and then supplied to XRD examination. A commercial  $\text{AlN}$  of 99.9% purity was purchased from Kojundo Chemical Laboratory.

Power X-ray diffraction (XRD) patterns were obtained with a RINT-2000 (Rigaku Denki) using Ni-filtered  $\text{Cu K}\alpha$  radiation. TG-DTA measurements were performed with a Mac Science 2000 apparatus in static air at a heating rate of  $10^\circ\text{C min}^{-1}$ .  $^{27}\text{Al}$  MAS NMR spectra were measured with a Bruker MSL-400 high-resolution NMR spectrometer, using magnetic field strength of 9.4 T, resonance frequency of 104.262 MHz, and spinning rate of 4 kHz. Chemical shifts were recorded with respect to an aqueous solution of  $\text{Al}(\text{H}_2\text{O})_6\text{Cl}_3$  used as an external standard. Raman spectra were obtained with a Jasco NRS-2000 spectrometer, using 514.5 nm line of an Ar laser of 200 mW power, collection of scattered light in a backscattering geometry, and multi-channel CCD detector.

### 3. Results and discussion

#### 3.1. Preparation of $(\text{Al}_2\text{OC})_{1-x}(\text{AlN})_x$ solid solution

Fig. 1 shows the X-ray diffraction patterns of the products, which were obtained just after the exothermic reactions, followed by the treatment in a 2 N HCl solution at  $80^\circ\text{C}$  for 2 h, and then by the controlled oxidation in air in a furnace at  $650^\circ\text{C}$  for 5 h, respectively. The as-prepared product (Fig. 1(a)) contains aluminum nitride, aluminum carbide and unreacted aluminum metal. In addition, the disappearance of

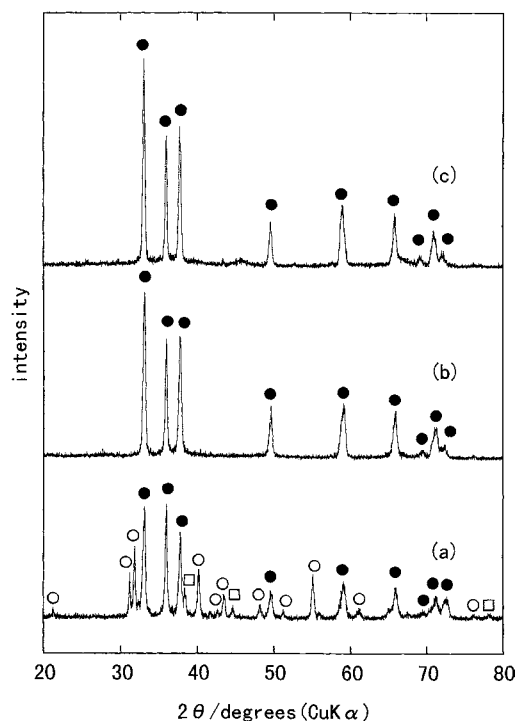


Fig. 1. XRD patterns for the products which were obtained (a) just after the exothermic reactions, and (b) after the treatment in a 2 N HCl solution at  $80^\circ\text{C}$  for 2 h, and then (c) after the oxidation in air at  $650^\circ\text{C}$  for 5 h. (●)  $(\text{Al}_2\text{OC})_{1-x}(\text{AlN})_x$ ; (○)  $\text{Al}_4\text{C}_3$ ; (□) Al.

graphite 0 0 2 line ( $2\theta = 26.36^\circ$ ) by grinding is observed, indicating the breaking of the ordered stacking of graphite layers and the formation of disordered carbon with fine particle size. After the treatment in a 2N HCl solution, aluminum carbide and unreacted aluminum metal were perfectly removed (Fig. 1(b)) and then disordered carbon was removed by the controlled oxidation in air at  $650^\circ\text{C}$  (Fig. 1(c)), as will be revealed in Fig. 2. Finally the product in Fig. 1(c) shows an almost single phase of aluminum nitride, though a trace of  $\eta\text{-Al}_2\text{O}_3$  is detected at  $2\theta = 45.5^\circ$ . The lattice constants calculated from these lines were  $a = 0.3130$  nm and  $c = 0.4993$  nm and lay between the values for AlN and  $\text{Al}_2\text{OC}$  having a wurtzite structure, indicating the formation of solid solution with the composition of  $(\text{Al}_2\text{OC})_{1-x}(\text{AlN})_x$ , where the  $x$ -value was estimated to be about 0.80 by assuming the validity of the Vegard rule.

Fig. 2 shows the Raman spectra of the samples obtained after the treatment in a 2 N HCl solution

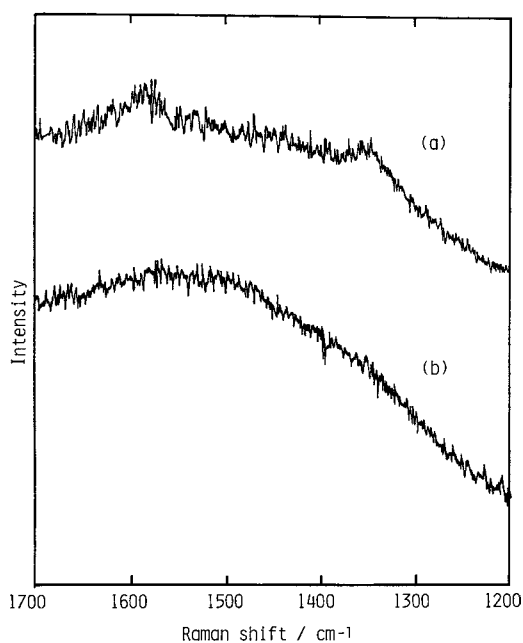


Fig. 2. Raman spectra of the samples obtained (a) after the treatment in a 2 N HCl solution at 80°C for 2 h and then (b) after the oxidation in air at 650°C for 5 h.

and then after the oxidation in air at 650°C, which correspond to the samples shown in Fig. 1(b) and (c), respectively. The former sample shows two broad peaks having comparable intensity at about 1580 and 1350  $\text{cm}^{-1}$  in Fig. 2(a), which are attributable to the disordered or amorphous carbon [13,14]. In fact, this result agrees with the disappearance of the 0 0 2 diffraction line of graphite after 30 min grinding as shown in Fig. 1(a). Tuinstra and Koenig [13] represented for the first time that a perfect crystal of natural graphite has a Raman band at 1575  $\text{cm}^{-1}$ , and a fine crystallite artificial graphite or glassy carbon has another band at 1355  $\text{cm}^{-1}$ . Furthermore, Nakamizo [14] studied the effect of grinding on the Raman spectra of Ceylon natural graphite, and reported that the intensity of 1360  $\text{cm}^{-1}$  band increased with an increase in grinding time and finally became larger than that of 1580  $\text{cm}^{-1}$  band after 200 h grinding, suggesting the formation of disordered carbon by long time-grinding. Thus, the sample shown in Fig. 2(a) was found to contain still disordered carbon which was formed by grinding. As shown in Fig. 2(b), however, after the oxidation in air at 650°C both bands

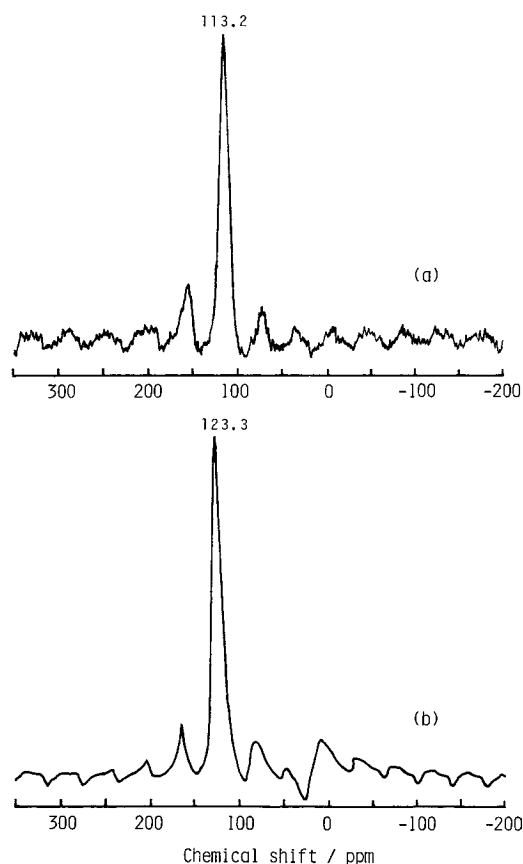


Fig. 3.  $^{27}\text{Al}$  MAS NMR spectra of (a) a commercial AlN and (b)  $(\text{Al}_2\text{OC})_{1-x}(\text{AlN})_x$  synthesized.

disappeared completely and the formation of disordered carbon-free  $(\text{Al}_2\text{OC})_{1-x}(\text{AlN})_x$  sample was confirmed.

Fig. 3 shows the  $^{27}\text{Al}$  MAS NMR spectra of a commercial AlN and disordered carbon-free  $(\text{Al}_2\text{OC})_{1-x}(\text{AlN})_x$  obtained by the controlled oxidation at 650°C in air. For a commercial AlN a central peak at 113.2 ppm and its spinning side bands are observed, which correspond to aluminum occupied octahedral sites of AlN lattice. The similar spectra are also obtained for the  $(\text{Al}_2\text{OC})_{1-x}(\text{AlN})_x$ , but the position of a central signal shifted to 123.3 ppm. The shift of the octahedral Al to 10 ppm lower magnetic field side for  $(\text{Al}_2\text{OC})_{1-x}(\text{AlN})_x$  is considered to be the effect of structural slightly different Al sites due to C and/or O dissolved into the AlN lattice.

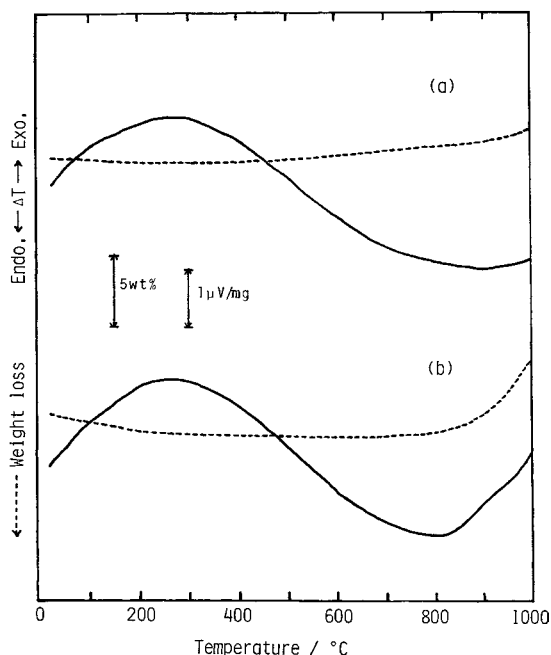


Fig. 4. TG–DTA curves for (a) a commercial AlN and (b)  $(\text{Al}_2\text{OC})_{1-x}(\text{AlN})_x$  synthesized in static air.

### 3.2. Oxidation behavior of $(\text{Al}_2\text{OC})_{1-x}(\text{AlN})_x$ and AlN

Fig. 4 shows the TG–DTA curves for a commercial AlN and  $(\text{Al}_2\text{OC})_{1-x}(\text{AlN})_x$  in static air. In a commercial AlN, a weight increase due to the oxidation is observed to start at temperatures above  $600^\circ\text{C}$ , followed by a very slow increase with increasing temperature up to  $1000^\circ\text{C}$ . The corresponding DTA curve shows the shift to the exothermic side at the beginning, to the endothermic side, and then the leveling at temperatures above  $800^\circ\text{C}$ . This tendency of the DTA curve agreed with that of the base-line obtained by using  $\alpha\text{-Al}_2\text{O}_3$  reference sample. A similar oxidation behavior is observed in  $(\text{Al}_2\text{OC})_{1-x}(\text{AlN})_x$  sample as well. A small weight loss of 1.3 wt% in early stage at temperatures below  $300^\circ\text{C}$  in TG curve may be attributable to adsorbed gases and/or water on the  $(\text{Al}_2\text{OC})_{1-x}(\text{AlN})_x$  sample, because this weight decrease changed by the heating of the sample at  $110^\circ\text{C}$  before the TG–DTA runs. Subsequently, a weight increase due to the oxidation starts at temperatures above  $700^\circ\text{C}$ , which is higher by  $100^\circ\text{C}$  than in a

commercial AlN. Once the weight increase initiates, in contrast with a commercial AlN, it was followed by a rapid increase at temperatures above  $850^\circ\text{C}$ , which also reflects in DTA curve shifting to exothermic side. The fractional conversion estimated by assuming the weight increase up to  $1000^\circ\text{C}$  in TG corresponding to the oxidation reaction of AlN or  $(\text{Al}_2\text{OC})_{1-x}(\text{AlN})_x$  to  $\text{Al}_2\text{O}_3$  was about 8% and 23%, respectively. In fact, the XRD patterns for the samples obtained after the heating up to  $1000^\circ\text{C}$  showed the presence of AlN alone in Fig. 4(a) and  $(\text{Al}_2\text{OC})_{1-x}(\text{AlN})_x$  with a small amount of  $\eta\text{-Al}_2\text{O}_3$  and a trace of  $\alpha\text{-Al}_2\text{O}_3$  in Fig. 4(b). Though it is not detected by XRD, the oxidation of a commercial AlN to fractional conversion of 8% seems to imply the formation of amorphous  $\text{Al}_2\text{O}_3$  or poorly crystallized  $\eta\text{-Al}_2\text{O}_3$  and/or oxynitrides. Actually, Azema et al. [15] also reports from an infrared spectroscopic study that the oxidation of AlN involves the formation of intermediate oxynitrides at temperatures as low as  $600^\circ\text{C}$ . In contrast with such a lower reactivity of a commercial AlN, the oxidation of  $(\text{Al}_2\text{OC})_{1-x}(\text{AlN})_x$  proceeded at a more rapid rate at temperatures above  $850^\circ\text{C}$  and attained higher fractional conversion of 23% at  $1000^\circ\text{C}$ . It can be expected that the higher reactivity of  $(\text{Al}_2\text{OC})_{1-x}(\text{AlN})_x$  depends on the essential effect of C and O dissolved in AlN lattice, causing a preferential oxidation of Al–C bonds in it and/or on the formation of porous, nonprotective  $\eta$ - and  $\alpha\text{-Al}_2\text{O}_3$  layer on it, not inhibiting further oxidation. Further study is needed to elucidate clearly the difference in the reactivity between  $(\text{Al}_2\text{OC})_{1-x}(\text{AlN})_x$  and AlN.

### References

- [1] J. Mukerji, in: C.N.R. Rao (Ed.), Nitride Ceramics, Blackwell Scientific Publications, Oxford, 1993, pp. 169.
- [2] T. Tsuchida, T. Hasegawa, M. Inagaki, J. Am. Ceram. Soc. 77(12) (1994) 3227.
- [3] T. Tsuchida, T. Kitagawa, M. Inagaki, Eur. J. Solid State Inorg. Chem. 32 (1995) 629.
- [4] T. Tsuchida, T. Hasegawa, Thermochim. Acta. 276 (1996) 123.
- [5] T. Tsuchida, T. Hasegawa, T. Kitagawa, M. Inagaki, J. Eur. Ceram. Soc. 17 (1997) 1793.
- [6] T. Tsuchida, T. Kitagawa, M. Inagaki, J. Mater. Sci. 32 (1997) 5123.
- [7] T. Tsuchida, Kawaguchi, M., Kodaira, K., Solid State Ionics 101–102, 103 (1997) 149.

- [8] T. Tsuchida, Y. Azuma, *J. Mater. Chem.* 7(11) (1997) 2265.
- [9] S.Y. Kuo, A.V. Virkar, *J. Am. Ceram. Soc.* 72(4) (1989) 540.
- [10] J. Edwards, K. Kawabe, G. Stevens, R.H. Tredgold, *Solid State Commun.* 3 (1965) 99.
- [11] J.M. Lihmann, T. Zambetakis, M. Daire, *J. Am. Ceram. Soc.* 72 (1989) 1704.
- [12] Y. Someno, T. Hirai, *Nippon Kinzoku Gakkai Kaihou* 30(11) (1991) 913.
- [13] F. Tuinstra, J.L. Koenig, *J. Chem. Phys.* 53 (1970) 1126.
- [14] M. Nakamizo, *Tanso* 90 (1977) 105.
- [15] N. Azema, J. Durand, R. Berjoan, C. Dupuy, L. Cot, *J. Eur. Ceram. Soc.* 8 (1991) 291.